J. Mater. Environ. Sci. 7 (7) (2016) 2424-2434 *Y. Filali Baba et al.*
ISSN : 2028-2508
CODEN: JMESCN

A study of 6- chloro-2-oxo-1,2-dihydroquinoline-4-carboxylic acid as new corrosion inhibitor for mild steel in hydrochloric acid solution

Y. Filali Baba[1], H. Elmsellem[2]*, Y. Kandri Rodi[1*], H. Steli[4], F. Ouazzani Chahdi[1], Y. Ouzidan[1], N. K. Sebbar[3], E. M. Essassi[3], K. Cherrak[2]

[1]*Laboratory of Applied Organic Chemistry, Faculty of Science and Technology, University Sidi Mohammed Ben Abdallah, Fez, Morocco.*
[2] *Laboratoire de chimie analytique appliquée, matériaux et environnement (LC2AME), Faculté des Sciences, B.P. 717, 60000 Oujda, Morocco*
[3]*Laboratoire de Chimie Organique Hétérocyclique, URAC 21, Pôle de Compétences Pharmacochimie, Mohammed V University, Faculté des Sciences, Av. Ibn Battouta, BP 1014 Rabat, Morocco.*
[4]*Laboratoire mécanique & énergétique, Faculté des Sciences, Université Mohammed Premier, Oujda, Maroc*.

**Corresponding author. E-mail :youssef_kandri_rodi@yahoo.fr / h.elmsellem@yahoo.fr*

Abstract

6- chloro-2-oxo-1,2-dihydroquinoline-4-carboxylic acid (P2) as a new corrosion inhibitor was synthesized in the present work. The corrosion inhibition of P2 in hydrochloric acid for mild steel was evaluated by potentiodynamic polarization measurements, electrochemical impedance spectroscopy, weight loss measurements, and DFT. The results indicate that the P1 is mixed type inhibitor, and the adsorption of P2 on mild steel surface obeys Langmuir isotherm. In addition, the inhibition efficiency increases with increasing the concentration of inhibitor and decreases with increasing the hydrochloric acid concentration. Correlation between quantum chemical calculations and inhibition efficiency of the investigated compound is discussed using the Density Functional Theory method (DFT).
Keywords: Mild steel, P2, Corrosion, Weight loss, Electrochemical, DFT.

1. Introduction

Here, we focus on the development of new chemically synthesized molecules which represents a major strategy for the discovery and preparation of new substances of biological interest. The quinolone derivatives are an important class of synthetic antibiotics known[1].They possess bactericidal activity [2-4].Several classes of organic compounds like quinolones are widely used as corrosion inhibitors for metals in acid environments [5-10](**Scheme 1**).

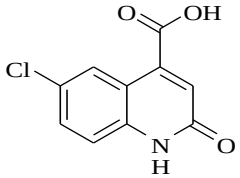

Scheme 1: 6- chloro-2-oxo-1,2-dihydroquinoline-4-carboxylic acid **(P2)**.

In this work, we investigate the corrosion of (MS) in 1 M HCl by **P2**.Weight loss tests and electrochemical techniques such as potentiodynamic polarization and electrochemical impedance spectroscopy have been used to study the effect of addition of this compound on the corrosion of steel in hydrochloric acid solution.

2. Experimental details

2.1. Synthesis of inhibitors

To a solution of 10 mmol of 5-chloro-isatin (P1) and 10 mmol of malonic acid in 30 ml of acetic acid was added 1 mmol of sodium acetate. The reaction mixture was refluxed for 24 hours. After cooling 100 ml of water-ice was added. The precipitate obtained was washed several times with ethanol.(**Scheme 2**):

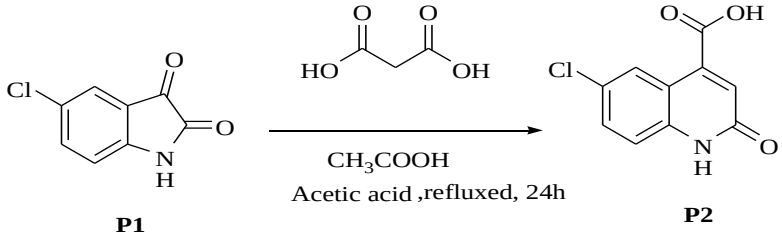

P1 **P2**

Scheme 2: Synthesis of 6- chloro-2-oxo-1,2-dihydroquinoline-4-carboxylic acid **(P2)**.

The analytical and spectroscopic data are conforming to structure of compound formed.
(P2): Yield= 83 % ; **Mp:** 655K **^{1}H NMR(300 MHz, CDCl$_3$) :** 6.91 (s, 1H,C**H**) ; 7.32 (d, 1H, 334 J_{H-H} = 9 Hz, (C**H** **arom**); 7.72 (d, 1H, J_{H-H} = 9 Hz, C**H$_{arom}$**); 8.22 (d, 1H, J_{H-H} = 1.8Hz, C**H**); 12.22(s, 1H, , N**H**) ; 14.05 (s, 1 H, O**H**). **^{13}C NMR(75 MHz, CDCl$_3$) :** 166.69 (**C**OOH), 161.24 (**C**=O), 139.64-138.7 (**Cq,Cq**), 131.14 (**CH$_{arom}$**), 126.7 (**CH$_{arom}$**), 126.07 (**CH**), 125.77 + (**CH$_{arom}$**), 118.08 (**C**q), 117.42 (**CH$_{arom}$**). **MassSpectrum (DIC / NH3)** : m/z = 223+[MH]

2.2. Materials and methods

The aggressive solutions of 1.0 M HCl were prepared by dilution of an analytical grade 37% HCl with double distilled water. Inhibitor solutions with concentrations of 10^{-6} to 10^{-3}mol dm^{-3} were employed for inhibition studies and were prepared by dissolving the required amount of (**P2**) in 100 mL of 1 M HCl by stirring at room temperature. 100 mL of 1 M HCl without inhibitor was used as blank test solution.
Coupons were cut into 1.5× 1.5 × 0.05 cm^3 dimensions having composition (0.09%P, 0.01 % Al, 0.38 % Si, 0.05 % Mn, 0.21 % C, 0.05 % S and Fe balance) used for weight loss measurements. Prior to all measurements, the exposed area was mechanically abraded with 180, 400, 800, 1000, 1200 grades of emery papers. The specimens are washed thoroughly with bidistilled water degreased and dried with ethanol. Gravimetric measurements are carried out in a double walled glass cell equipped with a thermostated cooling condenser. The solution volume is 50 cm^3. The immersion time for the weight loss is 6 h at (308±1) K. In order to get good reproducibility, experiments were carried out in duplicate. The average weight loss was obtained. The corrosion rate (*v*) is calculated using the following equation:

$$v = \frac{w}{st} (\mathbf{1})$$

Where: W is the average weight loss, S the total area, and t is immersion time. With the corrosion rate calculated, the inhibition efficiency (E_w) is determined as follows:

$$Ew\ \% = \frac{V_0 - V}{V_0} X\ 100 \quad (\mathbf{2})$$

Where: $\boldsymbol{v_0}$ and *v* are, respectively, the values of corrosion rate with and without inhibitor.
The electrochemical study was carried out using a potentiostat PGZ100 piloted by Voltamaster soft-ware. This potentiostat is connected to a cell with three electrode thermostats with double wall. A saturated calomel electrode (SCE) and platinum electrode were used as reference and auxiliary electrodes, respectively. Anodic and cathodic potentiodynamicpolarization curves were plotted at a polarization scan rate of 0.5mV/s. Before all experiments, the potential was stabilized at free potential during 30 min. The polarisation curves are obtained from −800 mV to −200 mV at 308 K. The solution test is there after de-aerated by bubbling nitrogen. Inhibition efficiency (E_p%) is defined as Equation (3), where $i_{corr}(0)$ and i_{corr}(inh) represent corrosion current density values without and with inhibitor, respectively.

$$E\mathrm{p}\% = \frac{\mathrm{icor}(0) - \mathrm{icor}(\mathrm{inh})}{\mathrm{icor}(0)} \mathrm{x}\ 100 \quad (\mathbf{3})$$

The electrochemical impedance spectroscopy (EIS) measurements are carried out with the electrochemical system, which included a digital potentiostat model Voltalab PGZ100 computer at E_{corr} after immersion in solution without bubbling. After the determination of steady-state current at a corrosion potential, sine wave voltage (10 mV) peak to peak, at frequencies between 100 kHz and 10 mHz are superimposed on the rest

potential. Computer programs automatically controlled the measurements performed at rest potentials after 0.5 hour of exposure at 308 K. The impedance diagrams are given in the Nyquist representation. Inhibition efficiency (E_R%) is estimated using the relation(4), where $R_{t(0)}$ and $R_{t(inh)}$ are the charge transfer resistance values in the absence and presence of inhibitor, respectively:

$$E_R\% = \frac{\mathrm{Rt(inh)} - \mathrm{Rt(0)}}{\mathrm{Rt(inh)}} \mathrm{x}\, 100 \qquad (\mathbf{4})$$

2.3. Quantum chemical calculations

All the quantum chemical calculations have been carried out with Gaussian 09 programmed package [11,12]. In our calculation we have used B3LYP, a hybrid functional of the DFT method, which consists of the Becke's three parameters; exact exchange functional B3 combined with the nonlocal gradient corrected correlation functional of Lee-Yang-Par (LYP) has been used along with 6-31G(dp) basis set. In the process of geometry optimization for the fully relaxed method, convergence of all the calculations has been confirmed by the absence of imaginary frequencies. The aim of our calculation is to calculate the following quantum chemical indices: the energy of highest occupied molecular orbital (E_{HOMO}), the energy of lowest unoccupied molecular orbital (E_{LUMO}), energy gap (ΔE), hardness (η),sotness (σ), electrophilicity index (ω), the fraction of electrons transferred (ΔN) from inhibitor molecule to the metal surface, and energy change when both processes occur, namely, and correlate these with the experimental observations.

The electronic populations as well as the Fukui indices and local nucleophilicities are computed using NPA (natural population analysis) [13–15]. Our objective, in this study, is to investigate computationally inhibitory action of quinoline derivative **P2** with chloridric acid in gas and in aqueous phase using B3LYP method with 6-31G(d,p) basis set.

- *Theory and computational details*

Theoretical study of benzothiazine derivative with chloridric acid as corrosion inhibitors was done by using the Density Functional Theory (DFT) with the B3LYP [16] /6-31G(d,p) method implemented in Gaussian 09 program package.

In this study, some molecular properties were calculated such as the frontier molecular orbital (HOMO and LUMO) energies, energy gap (E_{Gap}), charge distribution, electron affinity (A), ionization

Popular qualitative chemical concepts such as electronegativity [17, 18] (χ) and hardness [19] (η) have been provided with rigorous definitions within the purview of conceptual density functional theory(DFT) [20–22].

Using a finite difference method, working equations for the calculation of χ and η may be given as [20]:

$$\chi = \frac{I+A}{2} \text{or} \chi = -\frac{E_{HOMO} + E_{LUMO}}{2} \textbf{(5)}$$

$$\eta = \frac{I-A}{2} \text{or} \eta = -\frac{E_{HOMO} - E_{LUMO}}{2} \textbf{(6)}$$

Where I = $-E_{HOMO}$ and A= $-E_{LUMO}$ are the ionization potential and electron affinity respectively.

Local quantities such as Fukui function defined the reactivity/selectivity of a specific site in a molecule.

Using left and right derivatives with respect to the number of electrons, electrophilic and nucleophilic Fukui functions for a site k in a molecule can be defined [23].

$$f_k^+ = P_k(N+1) - P_k(N) \quad for\ nucleophilic\ attack \textbf{(7)}$$

$$f_k^- = P_k(N) - P_k(N-1) \quad for\ electrphilic\ attack \textbf{(8)}$$

$$f_k^+ = [P_k(N+1) - P_k(N-1)]/2 \quad for\ radical\ attack \textbf{(9)}$$

where, $P_k(N)$, $P_k(N+1)$ and $P_k(N-1)$ are the natural populations for the atom k in the neutral, anionic and cationic species respectively.

The fraction of transferred electrons ΔN was calculated according to Pearson theory [24]. This parameter evaluates the electronic flow in a reaction of two systems with different electronegativity, in particular case; a metallic surface (Fe) and an inhibitor molecule. ΔN is given as follows:

$$\Delta N = \frac{\chi_{Fe} - \chi_{inh}}{2(\eta_{Fe} + \eta_{inh})} \textbf{(10)}$$

whereχ_{Fe} and χ_{inh} denote the absolute electronegativity of an iron atom (Fe) and the inhibitor molecule, respectively; ηFe and ηinh denote the absolute hardness of Fe atom and the inhibitor molecule, respectively. In order to apply the eq.10 in the present study, a theoretical value for the electronegativity of bulk iron was used χ_{Fe} = 7 eV and a global hardness of η_{Fe} = 0, by assuming that for a metallic bulk I = A because they are softer than the neutral metallic atoms [24].

The electrophilicity has been introduced by Parr et al. [25], is a descriptor of reactivity that allows a quantitative classification of the global electrophilic nature of a compound within a relative scale. They have proposed the ω as a measure of energy lowering owing to maximal electron flow between donor and acceptor and ω is defined as follows.

$$\omega = \frac{\chi^2}{2\eta} \textbf{(11)}$$

The Softness σ is defined as the inverse of the η [26]

$$\sigma = \frac{1}{\eta} \textbf{(12)}$$

3. Results and Discussion

3.1. Weight loss measurements

3.1.1. Effect of inhibitor concentration

The weight loss method of monitoring corrosion rate is useful because of its simple application and reliability [27,28]. Therefore, a series of weight loss measurements were carried out after 6 h immersion in 1.0 M HCl in the absence and presence of various concentrations of the (**P2**). Table 1 shows the calculated values of corrosion rates obtained using Eq. (1) as well as inhibition efficiency values evaluated using the expression given in Eq. (2). The results show that the corrosion efficiencies for (P2) increase with increasing inhibitor concentration.

Table 1: Impedance parameters with corresponding inhibition efficiency for the corrosion of mild steel in 1.0 M HCl at different concentrations of (**P2**).

Inhibitor	**Concentration** (M)	**V** ($mg.cm^{-2}\,h^{-1}$)	**E_w** (%)
1M HCl	--	0.82	--
P2	10^{-6}	0.35	57
	10^{-5}	0.18	78
	10^{-4}	0.09	89
	10^{-3}	0.05	**94**

3.1.2.Adsorption isotherm and thermodynamicactivation parameters

The adsorption isotherm can be determined by assuming that inhibition effect is due mainly to the adsorption at metal/solution interface. Basic information on the adsorption of inhibitors on the metal surface can be provided by adsorption isotherm. In order to obtain the isotherm, the fractional surface coverage values (θ) as a function of inhibitor concentration must be obtained. The values of θ can be easily determined from the weight loss measurements by the ratio E_w%/100, where E_w% is inhibition efficiency obtained by weight loss method.

So it is necessary to determine empirically which isotherm fits best to the adsorption of inhibitor on the mild steel surface. Several adsorption isotherms (Frumkin, Langmuir, Temkin, and Freundlich) were tested. Data were tested graphically by fitting to various isotherms.

The plot of C_{inh}/θvs concentration of inhibitor (C_{inh}) produce a straight line with an approximately unit slope, indicating that the inhibitor under study obeys the Langmuir adsorption isotherm [29], as in the Eq. (13).

$$\frac{C}{\theta} = C + \frac{1}{K} \textbf{(13)}$$

Kads is the adsorption constant obtained from the intercept of the straight line. Eq. (14)give the association of the intercept of the straight line Kads with the standard free energy ΔGads

$$\Delta G_{ads} = -RT\ln[55.5K_{ads}] \quad \textbf{(14)}$$

Whereas R is the universal gas constant, the number 55.5 is the molar concentration of water in solution and T is the absolute temperature.

From Figure1we can calculate K_{ads} and ΔG_{ads}From Figure1 $\Delta G_{ads}$was calculated and it was −16.77 kJ/mol.

The negatively charge ΔG_{ads} elucidate the natural adsorption of the P2 on the mild steel surface and the vigorous interaction through the P2 and mild steel surface. Generally, if ΔG_{ads} is nearly −20 kJ/mol then it appropriate with physical adsorption, while if ΔG_{ads} nearly −40 kJ/mol then it is chemical adsorption occurring with the sharing of electrons from molecules of the inhibitor to the mild steel surface. In our work the ΔG_{ads} is around −40 kJ/mol and demonstrate mechanism of adsorption of P2 by means of chemical adsorption [30]. In hydrochloric acid solution the following mechanism is proposed for the corrosion of mild steel [31].

The anodic dissolution mechanism of mild steel is

$$Fe + Cl^{-} \leftrightarrow (FeCl^{-})_{ads}$$
$$(FeCl^{-})_{ads} \leftrightarrow (FeCl^{+})_{ads} + e-$$
$$(FeCl^{+})_{ads} \leftrightarrow Fe^{++} + Cl^{-}$$

The cathodic hydrogen evolution mechanism is

$$Fe + H^{+} \leftrightarrow (FeH^{+})_{ads}$$
$$(FeH^{+})_{ads} + e-(FeH)_{ads}$$
$$(FeH^{+})_{ads} + H^{+} + e^{-} \rightarrow Fe + H_2$$

Generally, the corrosion inhibition mechanism in an acid medium is adsorption of the inhibitor on the metal surface. The process of adsorption is influenced by different factors like the nature and charge of the metal, the chemical structure of the organic inhibitor and the type of aggressive electrolyte [32–34].

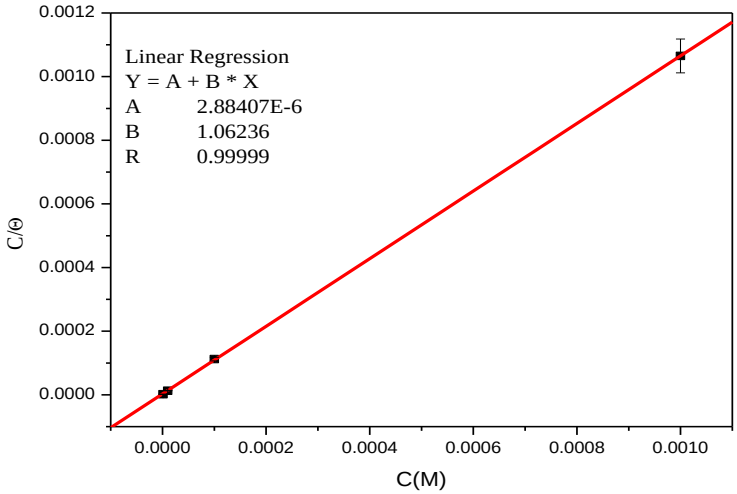

Figure1: Langmuir isotherm for the adsorption of P2 on the mild steel surface.

3.2. Polarization Measurements

Potentiodynamic polarization data of various concentrations of P2 is shown as the Tafel plots steel in 1 M HCl in Figure 2. The corrosion kinetic parameters such as corrosion potential (E_{corr}), corrosion current density (I_{corr}), cathodic Tafel slopes (β_c) were derived from this curve and are given in Table 2.

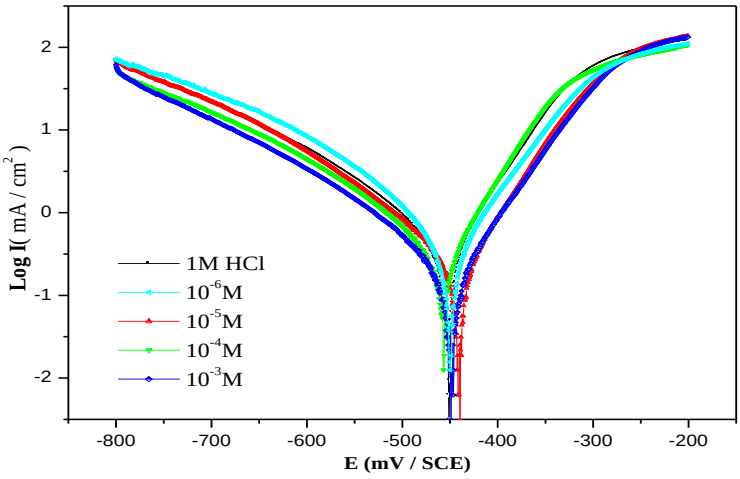

Figure**2:** Tafel plots of P2 in 1 M HCl.

Potentiodynamic polarization curves for mild steel in 1 M HCl solution at 308K without and with various concentration of P2 are presented in Figure 2. Since the largest displacement exhibited by P2 is 7 mV, P2 is

considered as a mixed-type inhibitor. Nevertheless, Figure 2 shows that the decreases in the anodic part are more pronounced than in the cathodic part, meaning that addition of P2 to 1 M HCl solution will reduce anodic dissolution of mild steel more than the cathodic hydrogen evolution reaction.

Table2: Potentiodynamic polarization parameters for the corrosion of mild steel in 1 M HCl solution containing different concentrations of P2 at 308K.

Inhibitor	**Concentration** (M)	**-E_{cor}** (V)	**β_C** (V/dec)	**I_{cor}** (mA/cm^2)	**Ep** (%)
1 M HCl	**--**	0,440	0,138	1.1951	--
P2	**10^{-6}**	0,462	0,169	0.4705	61
	10^{-5}	0,443	0,151	0.2167	82
	10^{-4}	0,438	0,136	0.1965	84
	10^{-3}	0,450	0,147	0.097	92

The data in Table 2 indicate that in both cases I_{corr} values gradually decreased with the increase of the inhibitor concentration with respect to the blank. Inhibition efficiency (Ep) at 10^{-3} M reaches up to a maximum of 92% which again confirm that both inhibitor is good inhibitor for mild steel in 1M HCl. According to the literature [35], it has been reported that (i) if the shift in E_{corr} is < 85 mV the inhibitor can be claimed as mixed type and (ii) if the shift in E_{corr} is > 85 mV, with repect to E_{corr}, the inhibitor behave as either cathodic or anodic. In this investigation, the shift in E_{corr} is less than 25 mV suggesting that both P2 act as mixed type of inhibitor[36].

3.3. Electrochemical impedance spectroscopy (EIS)

Electrochemical impedance spectroscopy study was undertaken to gain insight into the kinetics and characteristics of the electrochemical processes which occur at the MS / 1 M HCl interface in presence of the studied inhibitor (P2).Figure3 represent the Nyquist plots for mild steel dissolution in 1 M HCl in absence and presence of different concentration of the P2.

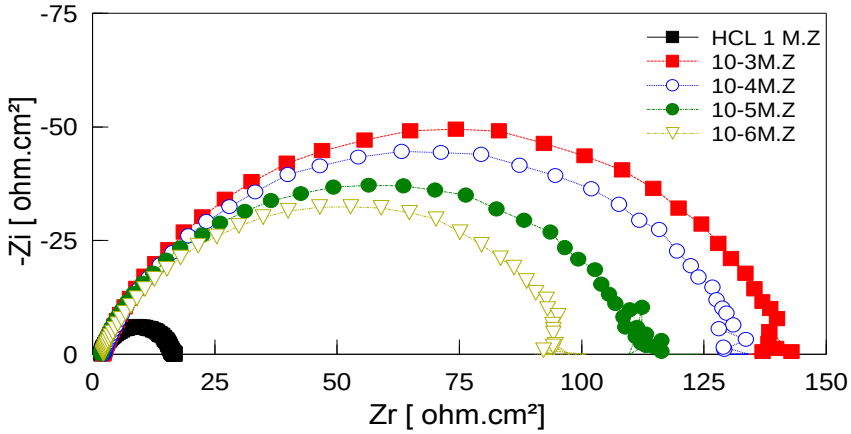

Figure3: Nyquist diagram for mild steel in 1 M HCl in the absence and presence of P2.

This finding also suggests that inhibition of metallic corrosion takes place by simple surface coverage mechanism. [37] The electrochemical impedance data was analyzed using the simple equivalent circuit of the form in Figure 5, which comprises the solution resistance (Rs), charge transfer resistance (Rct) and constant phase element (CPE). The use of CPE for acid based electrochemical corrosion of metals often yields better approximation. [38]

The imperfect semicircle of the Nyquist plots has been related to the deviation of *n* from unity (surface inhomogeneity), i.e. the pure capacitive behavior could not be achieved due to surface inhomogeneity caused by interfacial and structure origin.

The double layer capacitance was derived using the equation: [39]

$$C_{dl} = Y_0 (\omega_{max})^{n-1} \quad \textbf{(15)}$$

Where, ω_{max} (rad $^{s-1}$) is the angular frequency corresponding to the maximum value of imaginary impedance. Other EIS parameters such as R_s, R_{ct}, C_{dl}, and the corresponding inhibition efficiency (E_R(%)) are given in Table 3. The higher values of R_{ct} and lower values of C_{dl} in presence of P2 are attributed to increased surface coverage and decreased dielectric constant as well as thickness of the electric double layer, respectively.

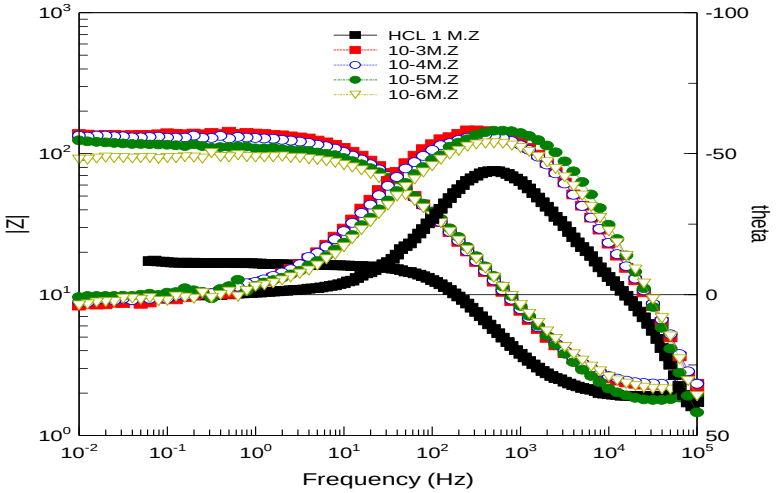

Figure4: Bode and phase plots of mild steel in 1.0 M HCl and in the presence different concentrations ofP2 at 308 K.

Table 3:Electrochemical parameters for mild steel in 1 M HCl without and with different concentrations of **(**P2**)** at 308K.

Concentration (M) / Prameters	**HCl 1M**	**10^{-6}**	**10^{-5}**	**10^{-4}**	**10^{-3}**
Real Center	9.25	48.41	58.64	66.95	70.16
Imag. Center	1.62	13.90	26.42	23.21	19.26
Diameter	15.13	95.56	126.59	137.19	140.18
Deviation	0.15	1.89	1.81	1.14	2.08
Low Intercept $R_s(\Omega.cm^2)$	1.86	2.69	1.12	2.41	2.77
High Intercept $R_t(\Omega.cm^2)$	16.64	94.12	116.16	131.50	137.56
Depression Angle	12.42	16.92	24.67	19.78	15.95
ω_{max}(rad s^{-1})	929.60	233.65	185.36	142.24	138.61
Estimated$R_t(\Omega.cm^2)$	14.78	91.43	115.04	129.09	134.79
Estimated $C_{dl}(F.cm^{-2})$	7.11 10^{-5}	4.47 10^{-5}	4.26 10^{-5}	3.12 10^{-5}	2.14 10^{-5}
E_R(%)	--	80	85	87	90

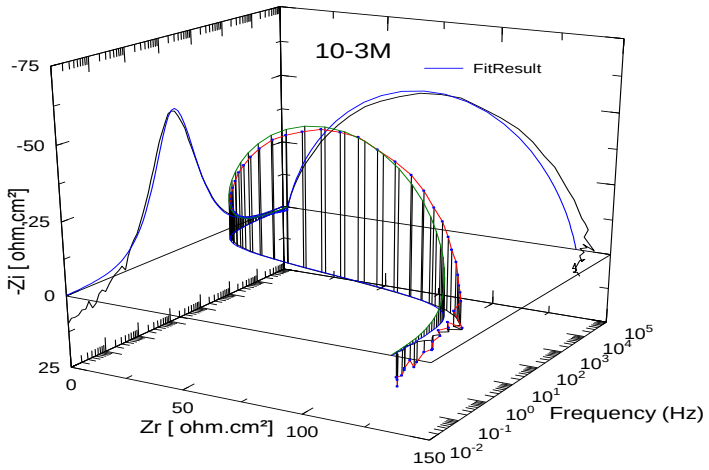

Figure 5: EIS Nyquist and Bode diagrams 3D for mild steel/1 M HCl + 10^{-3} M of **P2** interface: (------) experimental; (------) fitted data.

The increased surface smoothness is further supported by increased values of phase angle in the presence of inhibitor P2 as reflected in the Bode plots (Figure 4) and Table 3. The increased values of the slopes of the linear portion of the Bode impedance modulus plots at intermediate frequencies further support the formation of protective film of inhibitor molecules on the steel surface. More so, the closeness of the values of nto unity suggests that the CPE of the mild steel/electrolyte interface in the present study behaves as a pseudo-capacitor. The imperfect semicircle of the Nyquist plots has been related to the deviation of nfrom unity (surface inhomogeneity), i.e. the pure capacitive behavior could not be achieved due to surface inhomogeneity caused by interfacial and structure origin. Moreover, when a nonideal frequency response is present, it is commonly accepted to employ the distributed circuit elements in the equivalent circuits. What is most widely used is the constant phase element (CPE), which has a no integer power dependence on the frequency. Thus, the equivalent circuit depicted in Figure 6 is employed to analyze the impedance spectra Figure 5, where Rs represents the solution resistance,R_{ct}denotes the charge-transfer resistance, and a CPE instead of a pure capacitor represents the interfacial capacitance[40-41].

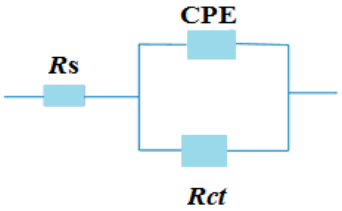

Figure 6. Equivalent circuit model used to fit the impedance spectra.

3.4. Theoretical study

3.4.1. Quantum chemical calculations

In the last few years, the FMOs (HOMO and LUMO) are widely used for describing chemical reactivity. The HOMO containing electrons, represents the ability (E_{HOMO}) to donate an electron, whereas, LUMO haven't not electrons, as an electron acceptor represents the ability (E_{LUMO}) to obtain an electron. The energy gap between HOMO and LUMO determines the kinetic stability, chemical reactivity, optical polarizability and chemical hardness–softness of a compound [42]. In this paper, we calculated the HOMO and LUMO orbital energies by using B3LYP method with 6-31G(d,p). All other calculations were performed using the results with some assumptions. The higher values of E_{HOMO} indicate an increase for the electron donor and this means a better inhibitory activity with increasing adsorption of the inhibitor on a metal surface, whereas E_{LUMO} indicates the ability to accept electron of the molecule. The adsorption ability of the inhibitor to the metal surface increases with increasing of E_{HOMO} and decreasing of E_{LUMO}. High ionization energy (I= 6.67 eV, I= 3.46 eV in gas and aqueous phases respectively) indicates high stability [43-45], the number of electrons transferred (ΔN) was also calculated and tabulated in Table 4.

Table 4. Quantum chemical descriptors of the studied inhibitor at B3LYP/6-31G(d,p) in gas, G and aqueous, A phases

Prameters	**Phase**	
	Gas	**Aqueous**
Total Energy *TE* (eV)	-30620.6	-30621.0
E_{HOMO} (eV)	-6.6752	-3.4679
E_{LUMO} (eV)	-0.4052	-1.3719
Gap ΔE (eV)	6.2700	2.0960
Dipole moment μ (Debye)	0.7504	1.3747
Ionisation potential I (eV)	6.6752	3.4679
Electron affinity A	0.4052	1.3719
Electronegativity χ	3.5402	2.4199
Hardness η	3.1350	1.0480
Electrophilicity index ω	1.9988	2.7939
Softness σ	0.3190	0.9542
Fractions of electron transferredΔN	0.5518	2.1852

The number of electrons transferred (ΔN) was also calculated and tabulated in Table 5. The ΔN(gas) < 3.6 and ΔN(aqueous) < 3.6 indicates the tendency of a molecule to donate electrons to the metal surface [46,47].

The calculated values of the f_k^+ for all inhibitors are mostly localized on the quinoline ring. Namely C_8, C_{12}, O_{14} and O_{17}, indicating that the quinoline ring will probably be the favorite site for nucleophilic attacks. The results also show that O_{14} atom is suitable site to undergo both nucleophilic and electrophilic attacks, probably allowing them to adsorb easily and strongly on the mild steel surface.

Table5: Pertinent natural populations and Fukui functions of the studied inhibitors calculated at B3LYP/6-31G(d,p) in gas, G and aqueous, A phases.

Atom k	*phase*	*P(N)*	*P(N+1)*	*P(N-1)*	f_k^+	f_k^-	f_k^0
C8	G	6,0916	6,2228	6,0912	0,1311	0,0005	0,0658
	A	6,1051	6,2302	6,0875	0,1251	0,0176	0,0713
C12	G	6,2361	6,3869	6,1922	0,1508	0,0439	0,0973
	A	6,2441	6,4099	6,1914	0,1658	0,0526	0,1092
O14	G	8,6031	8,6990	8,4208	0,0959	0,1823	0,1391
	A	8,6466	8,7352	8,4803	0,0886	0,1663	0,1275
O17	G	8,5093	8,6839	8,5616	0,1745	-0,0523	0,0611
	A	8,6126	8,7025	8,5947	0,0900	0,0178	0,0539

The final optimized geometries of P2 in gas and aqueous, selected valence bond angle and dihedral angles and bond lengths are given in Figure7. After the analysis of the theoretical results obtained, we can say that the molecule **P2** have a non-planar structure (Table 6).

Table 6 : The HOMO and the LUMO electrons density distributions of the studied inhibitors computed at B3LYP/6-31G (d,p) level in gas and aqueous phases.

	P2 Gas phase	**P2** Aqueous phase
HOMO	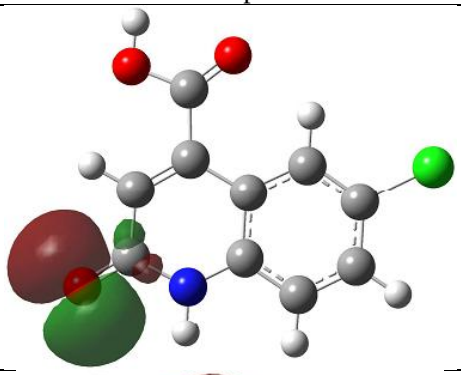	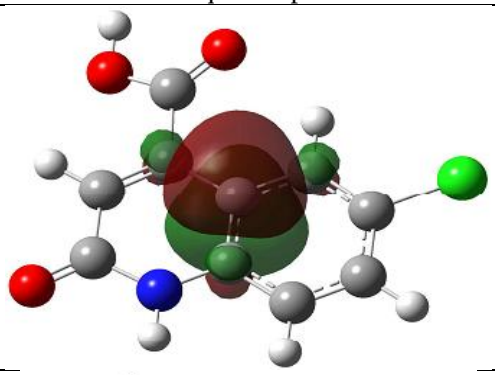
LUMO	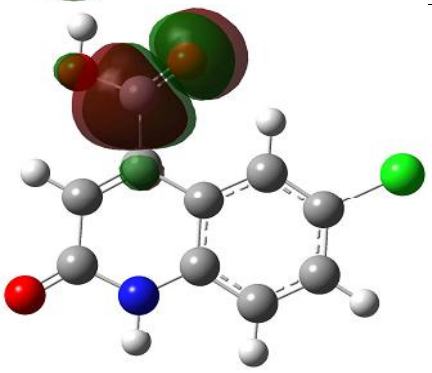	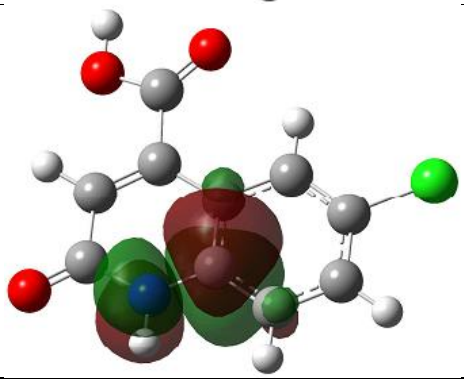

The inhibition efficiency afforded by the quinoline derivative P2 may be attributed to the presence of electron rich O.

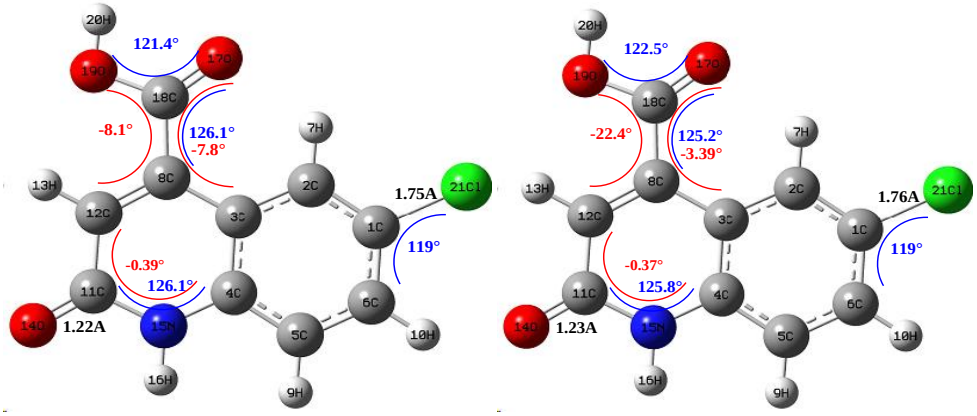

P2Gas phase **P2** Aqueous phase

Figure 7: Optimized molecular structures, selected dihedral angles (red), valence bond angle (blue) and bond lengths (black) of the studied inhibitors calculated in gas and aqueous phases at B3LYP/6-31G(d,p) levelof **P2**

Conclusion

The following conclusions may be drawn from the study:

- The inhibition efficiency of quinoline derivative (P2) for mild steel in HCl solution increases with increasing concentration.
- The corrosion current density significantly decreases and corrosion potential slightly changes with the addition of P2 in HCl solution, and the synthesized inhibitor of P2 is mixed type inhibitor.
- The adsorption of P2 on the mild steel surface obeys Langmuir isotherm.
- The presence of P2 in 1.0 M HCl solution increases charge transfer resistance, while it reduces double layer capacitance values. This result can be attributed to the increase of electrical double layer's thickness.
- The large efficiency of an inhibitor P2 is due to the presence of many atom of oxygen in this quinoline derivative. The calculated quantum chemical parameters such as HOMO-LUMO gap, E_{HOMO}, E_{LUMO}, dipole moment (μ) and total energy (TE) were found to give reasonably good correlation with the efficiency of the corrosion inhibition.

Reference

1. Naeem A., *Molecules*.21(2016)268.
2. Beruer H., *1ere éd. Edition la Pochothèque, France*. (2000) 411.
3. Yamamoto K., Irimura T., *Biochem J.*, 150 (2011) 477.
4. Khunt R., Datta N., Bharmal F., Rarikh A. R., *J. Ind. Chem. Soc*, 78 (2001) 47.
5. Eddy N.O. and OdoemelamS.A., *Adv. Nat. &Appl. Sci*. 2(1) (2008)35.
6. Obot I.B., Obi-Egbedi N. O., Umoren S.A., *Int. J. Electrochem. Sci*. 4 (2009) 863.
7. Ebenso E. E., Eddy N. O., Odiongenyi A. O., *Portugaliae Electrochimica. Acta*, 27(1) (2009) 13.
8. Eddy N.O., Ebenso E.E., *Int. J. Electrochem. Sci.* 5(2010)731.
9. Eddy N.O., *PhD Thesis,University of Calabar, Nigeria*,(2008).
10. Eddy N.O., OdoemelamS.A. and Mbaba A.J., *Afri. J. Pure & Appl. Chem*.2 (12)(2008)132.
11. Frisch M.J.,Trucks G.W.,Schlegeletal H.B., *Gaussian 09, Revision A.1, Gaussian, Inc.,Wallingford, Conn, USA*. (2009).
12. Elmsellem H., Youssouf M. H., Aouniti A., Ben Hadd T., Chetouani A., Hammouti B.. *Russian, Journal of Applied Chemistry*. 87(6) (2014) 744−753.
13. Li J., Li H., Jakobsson M., Li S., Sjodin P., Lascoux M., *Mol. Ecol*. 21 (2012) 28.
14. Hjouji M. Y., Djedid M., Elmsellem H., KandriRodi Y., Benalia M., Steli H., Ouzidan Y., OuazzaniChahdi F., Essassi E. M., and HammoutiB, *Der.Pharma.Chemica*. 8(4) (2016) 85-95.
15. Elmsellem H., Harit T., Aouniti A., Malek F., Riahi, Chetouani A., and HammoutiB., *Protection of Metals and Physical Chemistry of Surfaces*, A. 51(5) (2015)873–884.
16. Efil K. and BekdemirY., *Canadian Chemical Transactions*. 3(1) (2015) 85.
17. Pauling L., *3rd edn. Cornell University Press, Ithaca*. (1960).
18. Sen K.D., Jorgenson C., *Springer, Berlin.* 66 (1987).
19. Sen K.D., Mingos D.M.P., *Springer, Berlin*. 80 (1993).

20. Parr R.G., Yang W., *Oxford University Press,Oxford*. (1989).
21. Geerlings P., de Proft F., Langenaeker W., *Chem. Rev*.103 (2003) 1793.
22. Chermette H., *ComputJ..Chem*.20(1999)129.
23. Roy R.K., Pal S., Hirao K., *J. Chem. Phys*.110(1999)8236.
24. Pearson R.G., *Inorg. Chem*.27 (1988) 734.
25. Sastri, V.S. and Perumareddi, J.R., *Corrosion*. 53 (1997) 671.
26. Udhayakala P., Rajendiran T. V., and Gunasekaran S., *Journal of Chemical, Biological and Physical Sciences* A. 2(3) (2012) 1151–1165.
27. Elmsellem H., Aouniti A., Toubi Y., Steli H., Elazzouzi M., Radi S., Elmahi B., El Ouadi Y., Chetouani A., Hammouti B., *Der Pharma Chemica*. 7(7) (2015) 353-364.
28. Elmsellem H., Bendaha H., Aouniti A., Chetouani A., Mimouni M., Bouyanzer A., *Mor. J. Chem*. 2 (2014) 1-9.
29. Dandia A, Gupta L, Singh P, Quraishi MA. *Chem Eng.* 1 (2013)1303–1310.
30. Elmsellem H., Elyoussfi A., Steli H., Sebbar N. K., Essassi E. M., Dahmani M., El Ouadi Y., Aouniti A., El Mahi B., Hammouti B., *Der Pharma Chemica*. 8(1) (2016) 248-256.
31. Bavarian B, Kim Yeob, Reiner L.,*Corrosion.ApplElectrochem*. 34 (2003) 95.
32. Sebbar N. K., Elmsellem H., M. Ellouz, Lahmidi S., M. Essassi E., Fichtali I., Ramdani M., Aouniti A., Brahimi A.,Hammouti B., *Der Pharma Chemica*. 7(9) (2015) 33-42.
33. Al-Amiery AA, Kadhum AAH, Mohamad AB, *Junaedi S. Materials*. 6 (2013) 1420–1430.
34. Elmsellem H., Aouniti A., Khoutoul M., Chetouani A., Hammouti B., Benchat N., Touzani R. and Elazzouzi M., *Chem. J. Pharma.Res*. 6(4) (2014) 1216-1224.
35. Elmsellem H., Nacer H., Halaimia F., Aouniti A., Lakehal I., Chetouani A., Al-Deyab S. S., Warad I., Touzani R., Hammouti B. *Int. J. Electrochem. Sci*. 9 (2014) 5328.
36. Elmsellem H., Basbas N., Chetouani A., Aouniti A., Radi S., Messali M., Hammouti B., *Portugaliae. Electrochimica. Acta*. 2 (2014) 77.
37. Chevalier M.; Robert F.; Amusant N.; Traisnel M.; Roos C., Lebrini M. *Electrochim. Acta,* 13 (2014) 96.
38. Roy P.,Karfa P.,Adhikari U.,Sukul D.,*Corros. Sci*. 88 (2014) 246-253.
39. Yousefi A.,Javadian S.,Dalir N.,Kakemam J.,Akbari J.,*RSC Adv*. 5 (2015) 11697–11713.
40. Aouniti A., Elmsellem H., Tighadouini S., Elazzouzi M., Radi S., Chetouani A., Hammouti B., Zarrouk A., *Journal of TaibahUniversity for Science*. (2015).http://dx.doi.org/10.1016/j.jtusci.2015.11.008.
41. Elmsellem H., Karrouchi K., Aouniti A., Hammouti B., Radi S., Taoufik J., Ansar M., Dahmani M., Steli H. and El Mahi B., *Der.Pharma.Chemica*. 7(10) (2015) 237-245.
42. Govindarajan M., Karabacak M., *Spectrochim Acta Part A Mol BiomolSpectrosc*.85 (2012) 251–260.
43. Sikine M., KandriRodi Y., Elmsellem H., Krim O., Steli H., Ouzidan Y., KandriRodi A., OuazzaniChahdi F., Sebbar N. K., Essassi E. M., *J. Mater. Environ. Sci*.7 (4) (2016) 1386-1395.
44. Hjouji M. Y., Djedid M., Elmsellem H., KandriRodi Y., Ouzidan Y., OuazzaniChahdi F., Sebbar N. K., Essassi E. M., Abdel-Rahman I., Hammouti B., *J. Mater. Environ. Sci*. 7 (4) (2016) 1425-1435.
45. Chakib I., Elmsellem H., Sebbar N. K., Lahmidi S., Nadeem A., Essassi E. M., Ouzidan Y., Abdel-Rahman I., Bentiss F., Hammouti B., *J. Mater. Environ. Sci*. 7 (6) (2016) 1866-1881.
46. Lukovits I., Kalman E., Zucchi F., *Corrosion*. 57 (2001) 3-7.
47. Filali Baba Y., Elmsellem H., Kandri Rodi Y., Steli H., ADC., Ouzidan Y., Ouazzani Chahdi F., Sebbar N. K., Essassi E. M.,Hammouti B., *Der Pharma Chemica*, 8(4) (2016) 159-169.